arXiv:1606.06514v1 [cond-mat.mes-hall] 21 Jun 2016

Response of a spin valve to a spin battery

Khuôn-Viêt PHAM*
Laboratoire de Physique des Solides, Université Paris-Sud, Université Paris-Saclay, 91405 Orsay Cedex, France
(Dated: June 22, 2016)

It is shown that spin valves under suitable symmetry conditions exhibit an ON-OFF response to a spin battery, and are therefore perfect spin transistors. While a spin valve driven by a charge battery displays the usual GMR (Giant Magneto-Resistance), this means that a pure spin current or pure spin accumulation can generate an infinite magnetoresistance (IMR). Magnetic tunnel junctions as well as CPP (current perpendicular to plane) or CIP (current in plane) metallic trilayers are discussed.

PACS numbers: 85.75.-d; 75.47.-m; 73.43.Qt; 72.15.Gd; 73.50.Jt

I. INTRODUCTION. A THOUGHT EXPERIMENT

Giant Magneto-Resistance (GMR) has found ubiquitous use through spin valves[1,2]. The purpose of this paper is to investigate the response of a spin valve when one replaces a charge battery by a spin battery. Quite surprisingly the behavior of a spin valve driven by a spin battery differs markedly from the usual GMR.

A spin battery is any device which injects spin current into a load: it is therefore a spin current source. An alternative definition is to consider a spin battery as a spin accumulation source: in the standard drift-diffusion equations[3–6] the spin current density is indeed proportional to the gradient of the spin accumulation $j_s \propto \nabla(\mu_\uparrow - \mu_\downarrow)$. Since the spin accumulation in a given device will diffuse into any adjoining load, a spin current will also flow into the said load. In Johnson-Silsbee thermodynamic theory[4] as well as magnetoelectronic circuit theory for instance[7], spin accumulation acts as the spin analog of charge voltage and is a source for both charge and spin currents. A spin battery can thus be characterized by either the spin current it injects or its spin voltage (which we define as the spin accumulation recast in electrical units). Although this is obvious, this is a crucial remark for the argument which follows.

Let us sketch indeed with a simple resistor model why the response of a spin valve to a spin battery should be remarkable. Our argument will rely on considering a spin battery as a spin accumulation source. Fig.1 recalls for GMR the resistor analogy within an independent two-channel model for a CPP symmetric spin valve (ferromagnetic layers with the same material parameters, length, width ...). In Fig 1-(b), for anti-parallel magnetizations, each channel is subjected to the same (charge) voltage V_c. For a symmetric spin valve, currents flowing in each spin channel are equal $I_\uparrow = I_\downarrow$. The key observation is to ask what would happen if the spin channels had a reverse bias (opposite voltages) as in Fig. 2-(b) : the currents in each spin channel are now opposite $I_\uparrow = -I_\downarrow$; obviously no charge current can thus flow out of the device (since $I_c = I_\uparrow + I_\downarrow$) in contrast with what occurs in Fig.1 -(b) (GMR) and Fig.2-(a) (parallel case). But a reverse bias is precisely what a spin accumulation source can achieve: indeed a spin battery splits the chemical potentials for each spin channel $V_\uparrow \neq V_\downarrow$ and additionally $V_\uparrow = -V_\downarrow$ since $V_c = 0$ in the absence of a charge voltage applied to the system. It is easy to check that inclusion of a resistance for the normal layer does not change the conclusions. Replacing a charge battery with a spin battery therefore generates reversed biases and opposite currents in each spin channel (for a symmetric spin valve), so that in the anti-parallel state, there is no outgoing charge current: one has an infinite magnetoresistance or IMR.

In the previous discussion all magnetizations (in the spin battery and the spin valve) are supposed to share the same direction (collinear magnetizations) but we will also consider non-collinear situations.

This cartoon which assumes independent spin channels is quite simplistic: interface resistances at the contacts have been neglected, the spin accumulation at the detector (on the right in Fig. 2) is implicitly assumed to vanish while it actually extends throughout the device, voltage variations for each spin channels are implicitly linear in the resistor model while the spin accumulations relax exponentially; more importantly can the zero current survive in realistic conditions? One concern is the influence of the wiring either to the measurement apparatus or the battery: spin current leakage in the leads (or backflow in the spin battery) will indeed affect the signal in general. Another more serious issue which we will extensively discuss is the occurrence of offsets which plague non-local setups and shift the zero signal[8–16]. All these issues kill the IMR effect as a rule; nevertheless we will show that there exists symmetric setups with zero baselines thanks to a protection of IMR by symmetry. So although the resistor analogy is very limited, it does catch the essential physics of the IMR effect as will be shown in this paper.

Firstly we will discuss in Section II the origin of the IMR effect, which stems directly from the symmetry of response functions. We will introduce a variety of IMR effects (parallel IMR, anti-parallel IMR and non-collinear IMR). In Sections (III A-III C), we will consider various realizations (magnetic tunnel junctions and metallic trilayers) and propose experimental setups for testing our

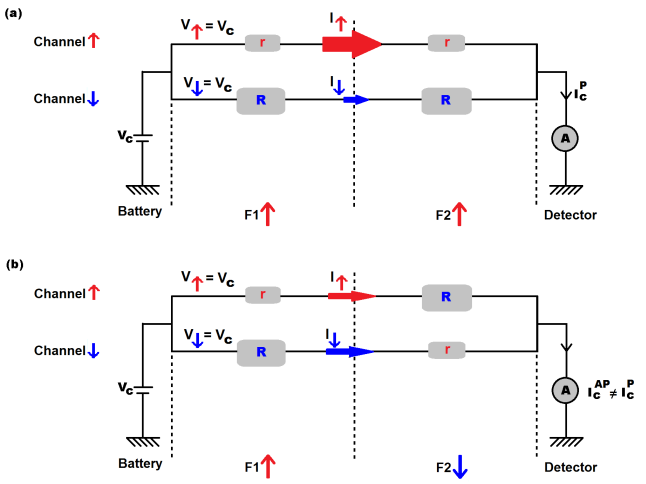

Figure 1. Color online. Equivalent resistor network for a CPP spin valve (standard GMR). The dashed line separates the ferromagnets (normal layer resistance neglected for simplicity). (a) Parallel magnetizations for the ferromagnets $F1$ and $F2$; (b) Anti-parallel magnetization with a larger resistance state.

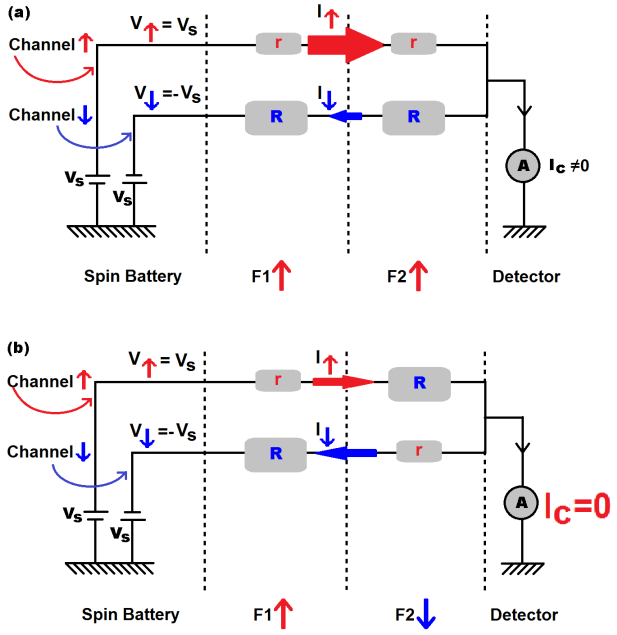

Figure 2. Color online. In the resistor network model, symmetric CPP spin valve driven by a spin battery which injects a spin current and induces spin accumulation. The latter is equivalent to reverse biasing the two spin channels. The currents (in electrical units) in each spin channel are $I_\uparrow$ and $I_\downarrow$. (a) Parallel magnetizations for ferromagnets $F1$ and $F2$: lower resistance state (larger current). (b) Anti-parallel magnetizations: current I_c at detector is vanishing since the currents in each channel are opposite. Therefore one has an infinite resistance state.

prediction of IMR.

II. SPIN BATTERIES AND GENERAL PROPERTIES OF TRANSPORT RESPONSE FUNCTIONS.

1. *Typical setups considered.*

We consider a spin battery connected to a magnetically active load. Since a spin accumulation appears in general in the load, a spin battery can be viewed as both a spin current source as well as a spin accumulation source.

Assumptions:

- we neglect spin backflow from the load to the battery. This is tantamount to using what we will define as *ideal spin batteries* which output either a constant spin current (ideal spin current source) or constant spin accumulation (ideal spin voltage source) *irrespective of the load*. **This hypothesis is not essential** and can be easily relaxed (see Section II 6 for a discussion of non-ideal batteries). We use it only for pedagogical reasons. These constant spin current or spin accumulation should be understood as evaluated at the connection from the battery to the load *on the side of the spin battery*. (If there is no spin-flip at the interface between the load and the battery, spin current is continuous but in general the spin accumulation is not continuous, hence the cautionary note.) A single spin battery connected to several loads through different connecting points will therefore deliver different spin voltages in general.

- Unless otherwise specified we further mostly restrict ourselves to **collinear setups** so that the spin accumulation in the battery has the same direction as the load magnetizations or spin accumulations.

In analogy to the voltage of a charge battery it is convenient to define a spin voltage in terms of chemical potentials for each spin species as:

$$V_s = -\frac{(\mu_\uparrow - \mu_\downarrow)}{2e} \tag{1}$$

which is just the spin accumulation of the spin battery recast in electrical units. The spin chemical potentials are evaluated locally in the battery at the exit point for the spin current (= entry point to the load).

We consider then a load connected to a spin battery and to two measurement leads: one has therefore a three-terminal setup since a spin battery is unipolar (Fig. 3). The spin battery acts as both a spin motive force and an electromotive force thanks to charge-spin coupling[4,17,18]. This means that in general a voltage drop between the two measurement terminals will appear (if the circuit is open) or a charge current (if the circuit is closed), both being proportional to the driving spin voltage. This basic setup can be reduced to a standard two-terminal setup if the wire connecting the spin battery to the load is also connected to the measurement apparatus (Fig. 3-(b)).

We will also discuss setups with two spin batteries driv-

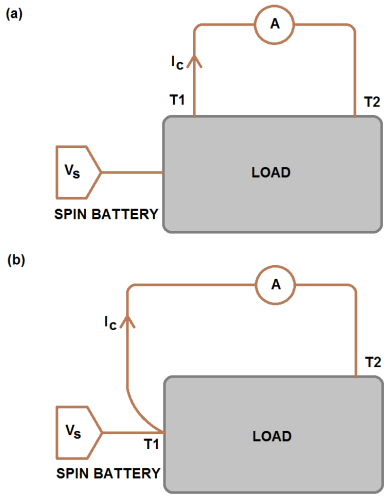

Figure 3. Color online. (a) A load driven by a spin battery (of spin voltage V_s) is in a 3-terminal geometry. For an open circuit between terminals $T1$ and $T2$, a voltage V_c is measured through charge-spin coupling due to a difference in spin accumulations at each terminal $T1$ and $T2$. For a closed circuit between $T1$ and $T2$ a charge current I_c is measured by the ammeter A. (b) Reduction to a two-terminal geometry when one measurement electrode merges with the battery terminal.

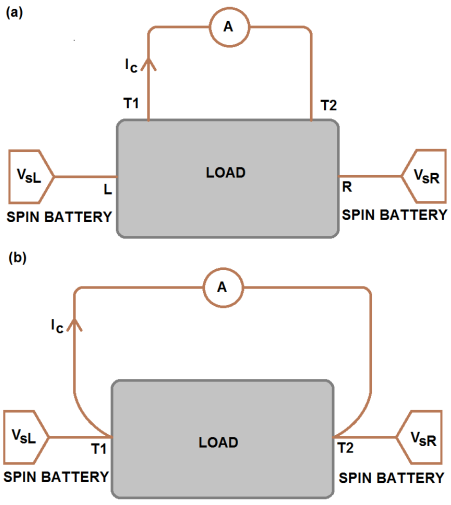

Figure 4. Color online. (a) A load driven by two spin batteries is in a 4-terminal geometry. (b) Reduction to a two-terminal geometry when the measurement electrodes $T1$ and $T2$ merge with the battery terminals L and R.

ing a load: we have then a four terminal geometry which can be reduced to a two-terminal one if measurement and batteries electrodes are merged (Fig. 4).

2. *Transport coefficients.*

Through Johnson-Silsbee charge-spin coupling[4,17,18] the measurement leads measure a charge response (a voltage in open circuit or a charge current if the circuit is closed). The charge response can be driven either by a spin current I_s or a spin accumulation (or spin voltage V_s). Within linear response this leads to the definition of several transport coefficients measuring the charge response to a spin drive:

$$g_{cs} = \frac{I_c}{V_s},\ r_{cs} = \frac{V_c}{I_s},\ h_{cs} = \frac{I_c}{I_s},\ k_{cs} = \frac{V_c}{V_s} \tag{2}$$

which have respectfully the dimensions of a conductance, a resistance or are dimensionless. We will name g_{cs} a 'charge-spin conductance'. While g_c is always positive, g_{cs} may be negative.

The spin response of the load can be defined as:

$$g_{ss} = \frac{I_s^{load}}{V_s} \tag{3}$$

where I_s^{load} is measured at the connection to the spin battery within the load (in general $I_s^{load} \neq I_s^{battery}$ if spin flip is not negligible at the load-battery interface). The multi-terminal geometry lends itself to defining other similar spin response coefficients dependent on the location of the spin current measured (for instance it might be at the measurement leads instead of at the battery).

Magnetization reversal. Let us suppose that the load comprises N magnetically active regions, whose **magnetizations are all parallel** and can be controlled independently. One can write therefore:

$$g_{cs} = g_{cs}\left(\sigma_1, \cdots, \sigma_N\right) \tag{4}$$

where $\{\sigma_1 = \pm 1, \cdots, \sigma_N = \pm 1\}$ index the magnetizations of the N regions relative to a given quantization axis.

It is clear that g_{cs} is an odd function of the $\{\sigma_i\}$:

$$g_{cs}\left(-\sigma_1, \cdots, -\sigma_N\right) = -g_{cs}\left(\sigma_1, \cdots, \sigma_N\right). \tag{5}$$

Indeed let us reverse all the spins (see Fig. 5): this is equivalent to reversing the quantization axis; therefore the charge current must be unchanged while the spin voltage is reversed $V_s \longrightarrow -V_s$, which proves Eq. (5). The other transport coefficients r_{cs}, h_{cs} and k_{cs} obey a similar relation. We refer to the examples in Sections III A - III C for explicit confirmations of such relations.

This is to be contrasted with the response to a charge battery $g_c = I_c/V_c$:

$$g_c\left(-\sigma_1, \cdots, -\sigma_N\right) = +g_c\left(\sigma_1, \cdots, \sigma_N\right) \tag{6}$$

which is even upon reversal of the magnetizations.

Charge voltage response. For a three terminal setup, the charge current flowing through the two measurement terminals (T_1 and T_2) is

$$I_c = g_c\, V_c + g_{cs}\, V_s \tag{7}$$

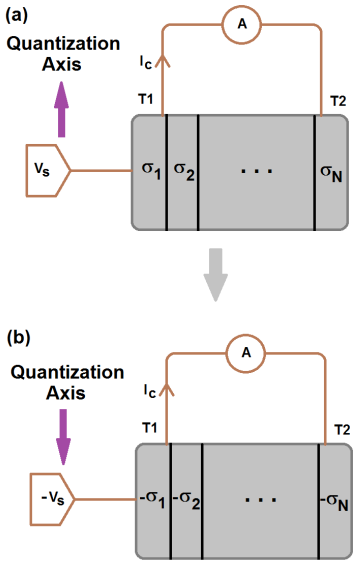

Figure 5. Color online. (a) Load with N collinear ferromagnets (e.g. multilayers); the directions of the magnetizations are indexed by $\sigma_i = \pm 1$ with a quantization axis indicated by the arrow. (b) If one flips the quantization axis, the charge current I_c is unaffected but $\sigma_i \longrightarrow -\sigma_i$ and $V_s \longrightarrow -V_s$. The response $\partial I_c/\partial V_s$ is therefore an odd function of σ_i $(i = 1...N)$.

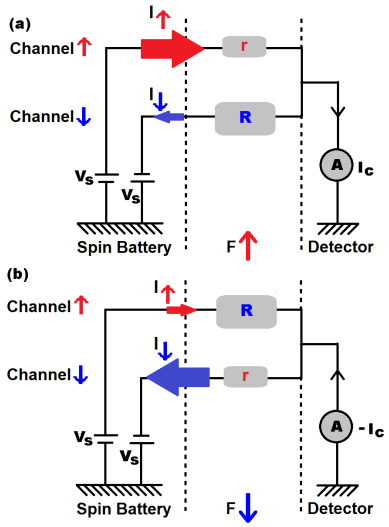

Figure 6. Color online. Ferromagnetic load connected to a spin battery in a two-channel model. The magnetization is reversed in (b) and therefore the current is also reversed.

where V_c is the voltage drop between terminals T_1 and T_2 and g_c is the two-terminal conductance between them. If T_1 and T_2 are shorted then $V_c = 0$ and one gets $I_c = g_{cs} V_s$; if the circuit is open between T_1 and T_2 then $I_c = 0$ and $V_c = -g_{cs}\, V_s/g_c$ which shows that

$$k_{cs} = -\frac{g_{cs}}{g_c}. \tag{8}$$

This simple relation allows translation of all the results of the paper in terms of charge voltages instead of charge currents. In practice it is probably better to measure a voltage response rather than a current response because this avoids Joule heating. For the sake of pedagogy we will stick to I_c and g_{cs} in what follows because the explicit calculations for real models in Sections III A - III C are mostly done for these quantities.

3. *Load with a single magnetically active region: Johnson bipolar transistor recovered.*

Let us reverse the magnetization of a single ferromagnetic layer connected to a spin voltage source V_s and to an ammeter (or voltmeter). Then from Eq. (5):

$$g_{cs}\,(-\sigma) = -g_{cs}\,(\sigma) \tag{9}$$

and therefore: $I_c \longrightarrow -I_c$. This proves quite generally that the response of a ferromagnet to a spin battery is bipolar.

It is instructive to consider a resistor network analogy. From Fig. 6, flipping the ferromagnet magnetization implies an exchange between the two channels: the channel currents which flow in opposite directions are therefore reversed, which results in a charge current reversal.

One has a bipolar response exactly as in the original Johnson bipolar transistor[10], which has just been deconstructed as a combination of a spin battery (a ferromagnetic layer in the original) and a ferromagnet acting as the load (see Fig. 7). Any spin battery could have been used instead of the single ferromagnet of Johnson original proposal.

One can deconstruct in a similar manner a CPP F1-N-F2 spin valve driven by a charge battery and consider F2 as a load driven by both a charge battery and a spin battery. Indeed the charge battery transforms F1 in a spin battery. The other layer F2 is then acted upon by both a charge battery and a spin battery. The spin battery induces a bipolar signal which is shifted away from zero due to the response to the charge battery which adds an offset. The signal is not bipolar anymore but is still bi-valued and depends on the ferromagnet polarization. This is the standard GMR (see Fig. 7).

In practice two factors have prevented Johnson bipolar transistor from reaching the domain of applications:

- offset voltages (or baseline voltages) shifting the signal $V_c' = V_c +$ offset and which have been credited to charge current inhomogeneities[8,11–13,19], or to heating (notably Joule and Peltier heating[14–16]).
- small signals, smaller usually than offset voltages, in the nV to $0.1\,mV$ range[10,20–22].

Offset voltages are by far the major nuisance. The main

advantage of using spin valves instead of a single magnetic layer is that setups without offset voltages can be devised as we will show later in this paper. This is why spin valves should be better candidates for practical applications than Johnson bipolar transistor.

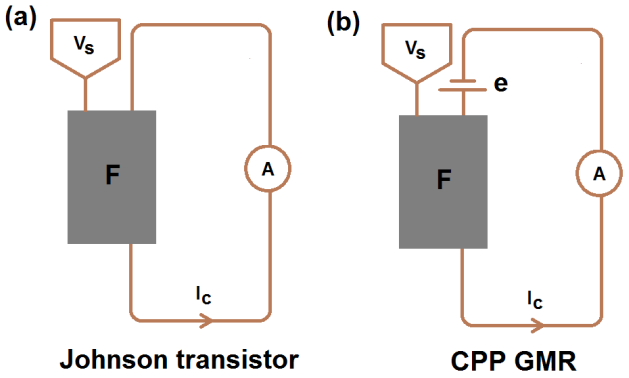

Figure 7. Color online. (a) Johnson transistor seen as a ferromagnet driven by a spin battery. (b) CPP GMR seen as a ferromagnet driven by both a charge battery and a spin battery.

4. Load with two magnetically active regions: IMR effect.

For a load with two magnetically active regions (such as an F-N-F trilayer), one has the general expression for the various response functions:

$$g\,(\sigma_1,\,\sigma_2) = g_0 + g_1\,\sigma_1 + g_2\,\sigma_2 + g_{12}\,\sigma_1\,\sigma_2. \qquad (10)$$

Since g_{cs} is an odd function of its arguments, this reduces to:

$$g_{cs}\,(\sigma_1,\,\sigma_2) = g_1\,\sigma_1 + g_2\,\sigma_2 \qquad (11)$$

while the charge conductance g_c is an even function of σ_i so that:

$$g_c\,(\sigma_1,\,\sigma_2) = g_0 + g_{12}\,\sigma_1\,\sigma_2. \qquad (12)$$

When one flips one of the two magnetizations, $|\Delta g_c| = 2\,|g_{12}|$ since $g_c = g_0 \pm g_{12}$. This is the GMR bi-valued response to a charge battery. The response to a spin battery is however four-valued as is obvious from Eq. (11) (see Fig. 8).

Bipolar response. Let us switch *both magnetizations*, then $g_{cs} \longrightarrow -g_{cs}$; or: $I_c \longrightarrow -I_c$. One recovers the bipolar behavior of the single layer.

Asymmetric valve. Let us examine what happens when one switches a single magnetization. As is obvious from Eq. (11) and Fig. 8, switching one of the two magnetizations can lead to a change of amplitude as in usual GMR but also a change of polarity (e.g. Fig. 8 Left: when going from ↑↑ to ↓↑).

Symmetric valve and Infinite magnetoresistance. Matters get more interesting if $|g_1| = |g_2|$

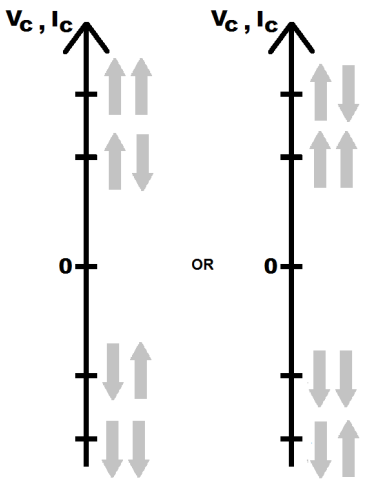

Figure 8. General response to a spin voltage for a system with two magnetically active regions: $g_{cs} = g_1\,\sigma_1 + g_2\,\sigma_2$. Flipping both magnetizations changes the sign of the measured signal (here either voltage $V_c = k_{cs}\,V_s$ or current $I_c = g_{cs}\,V_s$). Flipping a single one leads to a change of amplitude; according to the magnetization switched, additionally a change of polarity may occur. Left: g_1 and g_2 are positive. Right: $g_1 > 0$ but $g_2 < 0$ (and $g_1 > |g_2|$).

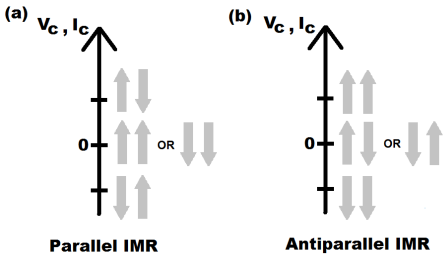

Figure 9. (a) Parallel IMR whereby IMR is achieved for parallel magnetizations; (b) anti-parallel IMR achieved for anti-parallel magnetizations.

which can occur if the system displays symmetries (see Fig. 9). Then upon switching a single layer, one has an ON-OFF effect since the response can vanish. Contrast in the signal becomes infinite. One has built a perfect spin transistor.

Parallel IMR: if $g_1 = -g_2$ then $g_{cs}(\sigma,\,\sigma) = 0$ so that the infinite resistance state corresponds to **parallel magnetizations** of the two regions (see Fig. 8-(a)). This is equivalent to requiring the symmetry

$$g_{cs}\,(\sigma_2,\,\sigma_1) = -g_{cs}\,(\sigma_1,\,\sigma_2) \qquad (13)$$

so that $g_{cs} = g_1 \times (\sigma_1 - \sigma_2)$. An obvious example is given in Fig. 10: one may think of a CPP symmetric trilayer with a spin battery connected to the central layer (see Fig. 10-(a) where the current flowing from terminals T_1 and T_2 is parallel to the layers), or of a non-local setup with two ferromagnetic regions (Fig. 10-(b)). Evidently

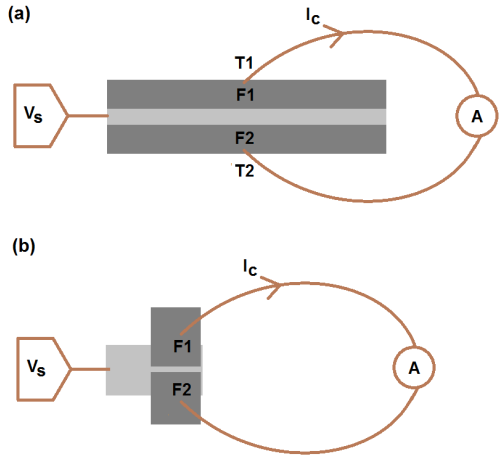

Figure 10. Color online. (a) Trilayer in CPP geometry (current flows perpendicularly to the layers from terminal T_1 to terminal T_2). The spin battery is attached to the central N layer. One has a parallel IMR since the state with parallel magnetizations has vanishing conductance. (b) Non-local setup analog of the top one.

the charge signal must vanish when the magnetizations are identical since the spin accumulations at each electrode $T1$ or $T2$ are equal. (For these setups Eq. (13) can be derived by noting that a π rotation around the N layer direction [horizontal in Fig. 10] amounts to exchanging F1 and F2 and reversing the current $I_c \longrightarrow -I_c$.)

Anti-parallel IMR: if $g_1 = g_2$ then $g_{cs}(\sigma, -\sigma) = 0$ so that the infinite resistance state corresponds to **anti-parallel magnetizations** of the two regions (see Fig. 8-b). The condition $g_1 = g_2$ is equivalent to having the symmetry

$$g_{cs}(\sigma_2, \sigma_1) = g_{cs}(\sigma_1, \sigma_2), \qquad (14)$$

which implies that $g_{cs} = g_1 \times (\sigma_1 + \sigma_2)$.This requirement means that the system (including the spin battery) must be invariant upon exchange of the two magnetically active regions, as viewed from the measurement electrodes (used as charge current or voltage probes). An example is a CIP trilayer with identical F layers (same dimensions, same material) and with the two measurement leads contacting both F layers in a symmetrical manner (see Fig. 11). The layers extend in a plane perpendicular to the plane of the picture; or more conveniently for experiments, the picture can also be seen to depict three parallel stripes so that the layers are in the same plane. Graphically it is obvious that an exchange of $F1$ and $F2$ must leave the charge current unchanged. Another example of setup obeying Eq. (14) is a symmetric CPP spin valve when spin-flip is negligible (see Appendix A).

Non-collinear IMR: For a non-collinear setup one has three directions to consider: $\mathbf{m_1}$, $\mathbf{m_2}$ the directions of the two magnetic regions within the load, $\mathbf{m}$ the direction within the spin battery of the spin accumulation; this allows to define a spin voltage vector as $\mathbf{V_{sL}} = \mathrm{V_{sL}}\,\mathbf{m}$

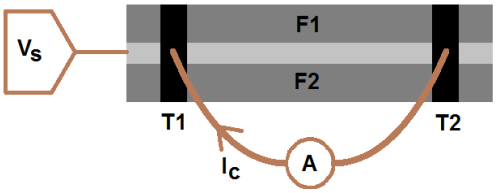

Figure 11. Color online. Trilayer or triple stripes in CIP geometry (current flows parallel to the layers between terminals T_1 and T_2). The spin battery must be connected symmetrically the central N layer. One has an anti-parallel IMR since the state with anti-parallel magnetizations has vanishing conductance.

for the spin battery. As an example we consider now the following non-collinear CPP geometry where $\mathbf{m_1}$, $\mathbf{m_2}$ are symmetric with respect to $\mathbf{m}$.

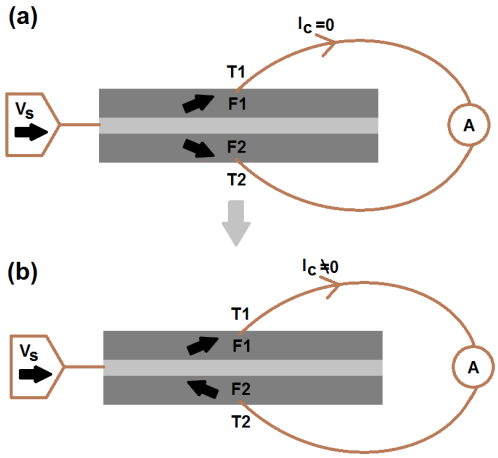

Figure 12. Color online. Non-collinear nanopillar. The arrow in the spin battery is the quantization axis for spin accumulation. (a) The ferromagnet magnetizations are non-collinear but symmetric with respect to the spin battery. Current vanishes by symmetry. (b) If one flips one of the magnetizations, symmetry is broken and current does not vanish any more.

Direct inspection of Fig. 12-(a) shows that by symmetry the current must vanish so that one has a non-collinear IMR. Note that the ferromagnet magnetizations can be out-of-plane with respect to the layers plane (as drawn in Fig. 12 so that it may be more appropriate to think of a nanopillar geometry), but an in-plane geometry is also possible. The symmetry argument is then a little bit different as shown on Fig.13 : if one rotates the setup around the direction of the spin voltage in the spin battery (that is, with respect to the central layer in Fig. 13), one exchanges the two ferromagnets, the current gets reversed $I_c \longrightarrow -I_c$; eventually, if the two ferromagnets are identical, one is back to the initial setup: the current therefore vanishes by symmetry. By design, offsets are therefore not possible in such a geometry.

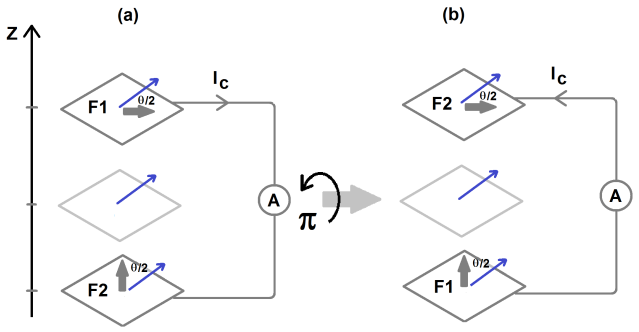

Figure 13. Color online. The setup is that of Fig.10-(a) but with in-plane non-collinear magnetizations. The thin arrow in each plane realls the direction of the spin voltage in the spin battery. The middle plane is a non-magnetic metallic layer. (a) The ferromagnet magnetizations are non-collinear but chosen symmetric with respect to the spin voltage direction. (b) If one makes a half-turn of the setup around the direction of the spin voltage in the central layer), one exchanges top and bottom so that the current gets reversed. If the layers $F1$ and $F2$ are identical, one ends up with the initial setup: the current must therefore vanish by symmetry.

Comparison with GMR for a spin valve driven by a charge battery: in order to achieve an infinite magnetoresistance with a charge battery (for which $g_c\,(\sigma_1,\,\sigma_2) = g_0 + g_{12}\,\sigma_1\,\sigma_2$) it would be necessary that $|g_0| = |g_{12}|$. This is a condition which is more difficult to achieve than relying on geometrical symmetries of the setup. For instance for magnetic tunnel junctions, Jullière classic result translates into: $g_{12} = g_0\,P^2$ where $P = |n_\uparrow - n_\downarrow|\,/\,(n_\uparrow + n_\downarrow)$ is the (absolute value of the) density of states polarization. In order to achieve the condition $g_0 = \pm g_{12}$ one needs to have $P = \pm 1$, that is perfect polarization of each layer, or half-metals. This is in contrast with the IMR due to spin batteries: one does not need half-metallic layers acting as perfect spin filters. The essence of spin battery driven IMR is not spin filtering by magnetic layers but combines the pseudo-vector nature of magnetic fields and magnetizations with geometrical symmetries. This is an important distinction to bear in mind.

Offsets: much as the bipolar transistor or non-local spin valve are parasitized by baseline voltages, the IMR effect can be likewise spoiled by offset currents (or voltages if a voltmeter replaces the ammeter). However symmetry can protect many of these setups. As an illustration, in the CPP setup of Fig. 10 there can be by design **no offsets** when ferromagnets $F1$ and $F2$ have parallel magnetizations: the voltage obviously vanishes due to the geometry. This is not the case of the CIP setup in Fig. 11 although this is easily remedied as we next show.

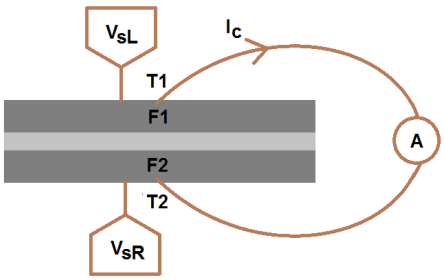

Figure 14. Color online. Symmetric trilayer in CPP geometry connected to two spin batteries (in a symmetrical manner). For identical spin voltages, one has a parallel IMR while for opposite spin voltages, one has an anti-parallel IMR

5. *Connecting two spin batteries to a load with two magnetically active regions.*

We turn to a four-terminal geometry with two spin batteries with spin voltages V_{sL} and V_{sR} at terminals L and R while the charge response is measured at terminals T_1 and T_2 (see Fig. 4). Quite generally one expects the following relation from linear response:

$$I_c = g_c\,V_c + g^L_{cs}\,V_{sL} + g^R_{cs}\,V_{sR} \tag{15}$$

where as before V_c is the voltage drop between T_1 and T_2. Previous properties for a single spin battery generalize in a straightforward manner: the charge-spin conductances are odd functions of magnetization $g^{L/R}_{cs}(-\sigma_1,\,-\sigma_2) = -g^{L/R}_{cs}(\sigma_1,\,\sigma_2)$.

General case. If offsets can be neglected or are small enough then it becomes possible to generate an IMR without any symmetry requirement on the load. The second spin voltage allows us to cancel out both the offsets and the response to the first spin battery by calibrating it to that end. One can achieve both anti-parallel and parallel IMR as well as non-collinear IMR.

- **Anti-parallel IMR:** in the absence of any offsets, for $\sigma_2 = -\sigma_1$, provided V_{sR} is chosen as

$$V_{sR} = -g^L_{cs}(\sigma_1,\,-\sigma_1)\,V_{sL}/g^R_{cs}(\sigma_1,\,-\sigma_1), \tag{16}$$

  then trivially $I_c(\sigma_1,\,-\sigma_1) = 0$ while in general $I_c(\sigma_1,\,\sigma_1) \neq 0$. If there is a small offset, one just adjusts V_{sR} to cancel it in order to achieve IMR. As an example, let us consider the symmetric CPP setup of Fig. 14 for which one has the relation $g^L_{cs}(\sigma_1,\sigma_2) = -g^R_{cs}(\sigma_2,\sigma_1)$ which follows from symmetry (by exchanging L and R in Fig. 14, the current $I_c \longrightarrow -I_c$ while $V_{sL} \longrightarrow V_{sR}$ and $\sigma_1 \longrightarrow \sigma_2$); this implies that the condition for anti-parallel IMR becomes $V_{sR} = -g^L_{cs}(\sigma_1,\,-\sigma_1)\,V_{sL}/g^R_{cs}(\sigma_1,\,-\sigma_1) = -V_{sL}$, therefore $V^R_s = -V^L_s$.

- **Parallel IMR:** in the absence of any offsets, for $\sigma_2 = \sigma_1$, provided V_{sR} is chosen as

$$V_{sR} = -g^L_{cs}(\sigma_1,\,\sigma_1)\,V_{sL}/g^R_{cs}(\sigma_1,\,\sigma_1), \tag{17}$$

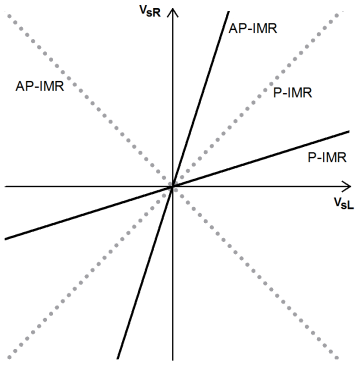

Figure 15. Color online. The relations between the spin voltages required to achieve IMR are linear (AP: anti-parallel, P : parallel); the dotted lines correspond to the setup of Fig. 14 ($V_{sL} = \pm V_{sR}$).

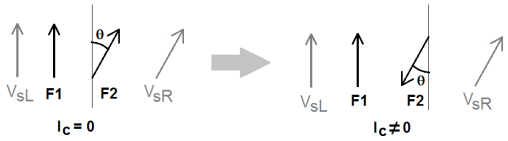

Figure 16. Color online. Non collinear IMR occurs for non-collinear magnetizations; upon switching of one of the magnetizations (which remain non-collinear) one has an IMR. Left: one of the spin voltages is adjusted to achieve a zero signal. Right: the previous adjustment does not work if we change the relative directions of the ferromagnets.

then $I_c(\sigma_1,\, \sigma_1) = 0$ while in general $I_c(\sigma_1,\, -\sigma_1) \neq 0$. For the symmetric CPP setup of Fig. 14 the condition reduces to $V_s^R = V_s^L$. The two conditions Eq. (16-17) are shown in Fig. 15.

- **Non-collinear IMR.** For a non-collinear setup one has four directions to consider: $\mathbf{m_1}$, $\mathbf{m_2}$ the directions of the two magnetic regions within the load, $\mathbf{V_{sL}}$ and $\mathbf{V_{sR}}$ the spin voltage vectors for each spin battery giving the directions of the spin accumulations they generate. As an example we consider now the following non-collinear setup where each of the two magnetic region is locked to one of the spin batteries so that $\mathbf{m_1} \parallel \mathbf{V_{sL}}$ and $\mathbf{m_2} \parallel \mathbf{V_{sR}}$ but there is an angle $\theta = (\mathbf{m_1},\, \mathbf{m_2})$ (see Fig. 16 but other configurations are of course possible). The condition to achieve IMR for angle θ is then simply:

$$V_{sR} = -g_{cs}^L(\theta)\, V_{sL}/g_{cs}^R(\theta). \tag{18}$$

This much enlarges the scope of IMR by providing applications to angular sensors for instance. In practice the observability of these IMR effects much depends on the ability to control the amplitude of the offsets; although it might be possible in the future to achieve an electrical control of them, it is much simpler to consider setups where offsets cancel out by symmetry.

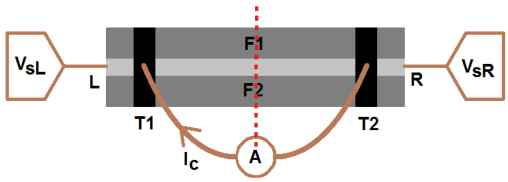

Figure 17. Color online. Symmetric layers or stripes in CIP geometry hooked to two spin batteries (in a symmetrical manner). For opposite spin voltages it can be shown that one has an anti-parallel IMR. (The dashed line indicates a plane of symmetry exchanging left and right spin batteries.)

Offset-free setups.

- **symmetric CIP geometry.** Some relations can be found between the two conductances g_{cs}^R and g_{cs}^L for special setups; an example is the symmetric CIP setup in Fig. 17 for which $g_{cs}^L = -g_{cs}^R$ because of a plane of symmetry (dashed line in Fig. 17): indeed under reflection through that plane $I_c \longrightarrow -I_c$ while $V_{sL} \longrightarrow V_{sR}$. Furthermore the relation found for a single spin battery can be generalized $g_{cs}^{L/R}(\sigma_1,\, \sigma_2) = g_{cs}^{L/R}(\sigma_2,\, \sigma_1)$ since the exchange of ferromagnetic layers can not change the response if they are identical. If we combine with $g_{cs}^L = -g_{cs}^R$ then $I_c\,(\sigma_1,\, -\sigma_1) = g_{cs}^L\,(\sigma_1,\, -\sigma_1)\,(V_{sL} - V_{sR}) = 0$. One has an anti-parallel IMR but notice that in this argument there is no condition imposed on the spin voltages which might be arbitrary, if offsets are discounted. To avoid offsets and enable IMR, it is necessary to choose special values of the spin voltages, namely $V_{sL} = -V_{sR}$. Indeed let us inspect Fig.18; a spin voltage $-V_{sL}$ at the right spin battery is equivalent to a spin voltage $+V_{sL}$ as measured against the opposite quantization axis. If we then make a half-turn, exchanging left and right, the current is reversed. But the rotated setup is actually identical to the initial one provided the CIP layers are identical. Therefore the current must identically vanish. Therefore there can be no offsets for such a symmetric CIP spin valve with symmetric spin batteries. Note that Fig.17 can be thought of as a layered geometry (parallel planes perpendicular to the Figure as in standard CIP GMR) or one where the layers are actually in the picture plane (three parallel stripes) so that our discussion equally applies to layers or stripes.

- **symmetric CPP geometry.** Symmetric CPP trilayers (identical ferromagnetic layers, identical spin batteries, symmetric wiring, see Fig. 19) obey the obvious relation $g_{cs}^L(\sigma_1,\, \sigma_2) = -g_{cs}^R(\sigma_2,\, \sigma_1)$ which follows from exchanging the ferromagnetic layers and the spin batteries attached to them. Therefore $I_c\,(\sigma_1,\, -\sigma_1) =$

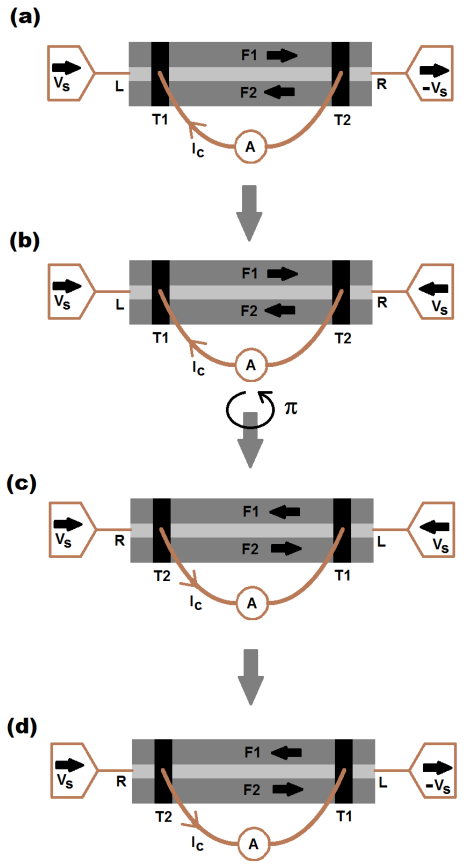

Figure 18. Color online. (a) CIP symmetric spin valve subjected to opposite spin voltages; for the ferromagnets, the arrows indicate the magnetization direction while for the batteries they correspond to the reference direction against which the spin accumulation $(\mu_\uparrow - \mu_\downarrow)$ is measured. (The black bars labelledT_1 and T_2 depict the contact with the current measurement wires and the two measurement terminals.) (b) A negative spin voltage is equivalent to a positive one for the reversed quantization axis. (c) Setup after a half-turn which exchanges left and right . (d) The current is reversed after these operations. The position of $F1$ and $F2$ as top or bottom layers is immaterial. The bottom setup is therefore equivalent to the top one with the current reversed *if the layers are identical*. The current must therefore vanish by symmetry.

$g^L_{cs}(\sigma_1, -\sigma_1)(V_{sL} + V_{sR})$ which vanishes for $V_{sL} = -V_{sR}$ (anti-parallel IMR) while $I_c(\sigma_1, \sigma_1) = g^L_{cs}(\sigma_1, \sigma_1)(V_{sL} - V_{sR})$ is non vanishing unless $V_{sL} = V_{sR}$ (parallel IMR). These are the conditions quoted above for parallel and anti-parallel IMR (discussion below Eq. (16) and Eq. (17) and Fig. 15). *These derivations are valid only if offsets are negligible.* However it can be shown directly that for the symmetric spin voltages $V_{sL} = -V_{sR}$ or $V_{sL} = V_{sR}$ there can be no offsets for respectively anti-parallel and parallel alignment of the magnetizations.

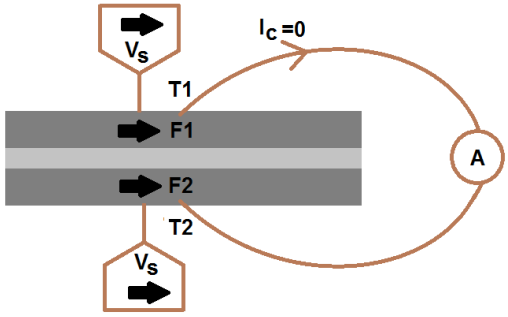

Figure 19. Color online. Parallel IMR for a symmetric CPP trilayer: the obvious symmetry ensures the current vanishes and that there is no offset.

- Indeed for identical spin voltages $V_{sL} = V_{sR}$ and parallel magnetizations, direct inspection of Fig. 19 shows that there can not be any privileged direction for the current which therefore vanishes: one has therefore a parallel IMR.

- Additionally for opposite spin voltages $V_{sL} = -V_{sR}$ symmetry again enforces a vanishing current and zero offsets as can be seen by inspecting Fig. 20. A right spin voltage $-V_s$ is equivalent to a spin voltage $+V_s$ measured against the opposite direction for the magnetization. If we make a half-turn within the the plane of the Figure, the current gets reversed while there is a top-bottom exchange (Fig. 20-(c)). If the layers are identical, one ends up in Fig. 20-(d) with a setup identical to the initial one but with a reversed current. The latter must therefore vanish by symmetry and there can be no offsets.

- Offset-free non-collinear IMR can also be enforced by tilting the magnetizations in a symmetrical manner as in Fig. 21. The magnetizations are supposed to be in-plane but out-of-plane setups (nanopillars) are clearly possible to achieve offset-free non-collinear IMR.

6. *Spin backflow, interface resistance and spin leakage; practical considerations.*

The previous discussions can easily include spin backflow and non-ideal spin batteries (spin batteries whose spin voltage depends on the load). In the frame of linear response a simple argument shows that the IMR effect will remain. Indeed a non-ideal spin voltage source will output a decreased spin voltage; this means that the HIGH signal will decrease by some factor r, but since the LOW signal vanishes, the obvious algebra $0 = 0 \times r$ implies that one still has an IMR although the contrast is decreased (ΔX is smaller, where X is the measured signal, either a voltage or a current). This simple argument

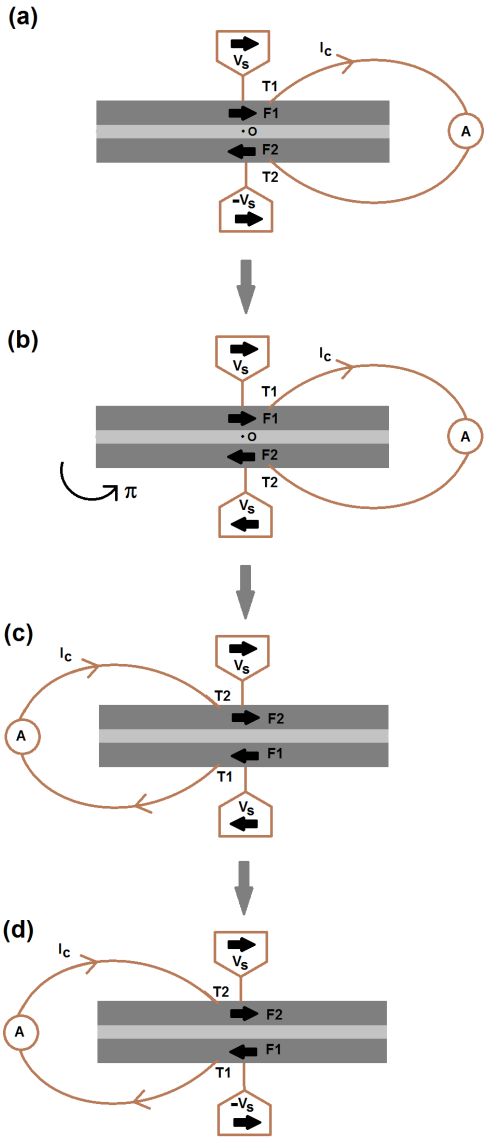

Figure 20. Color online. (a) Symmetric CPP trilayer subjected to opposite spin voltages relative to the direction indicated on the spin batteries. (b) A negative spin voltage is equivalent to a positive one for the reversed reference direction. (c) setup after a half-turn in the Figure plane around the center of the layers (O). (d) The setup of (a) is recovered but with an opposite current: the current therefore vanishes.

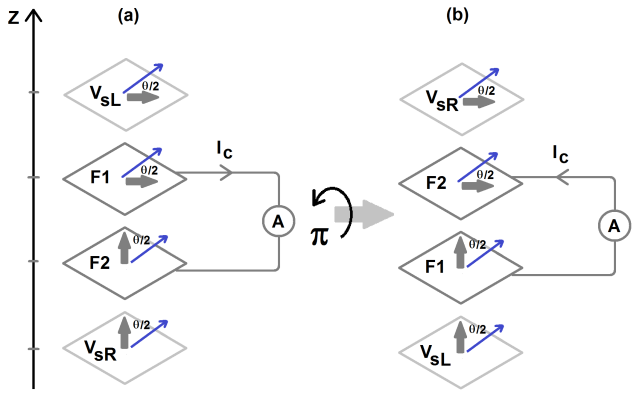

Figure 21. Color online. (a) Symmetric CPP trilayer. The thick arrows correspond to the directions of the (in-plane) magnetizations (of the ferromagnets or of the spin voltages). The top (resp. down) spin voltage and ferromagnets have the same directions. (b) After a half-turn, top and bottom are exchanged and current I_c is reversed. If V_{sR} is chosen equal to V_{sL} one ends up with the initial setup albeit with a reversed current. Therefore the current vanishes.

can be put on firmer grounds if one introduces the concept of an *internal spin resistance* r_{IS} which is the analog of the internal resistance of charge batteries and relates spin voltage and spin current through a linear relation[23].

It is also straightforward to include the effects of interface resistances between the spin battery and its load. In terms of both an internal spin resistance of the spin battery (which regulates spin backflow) r_{IS} and an interface resistance r_c, the end-result is a simple renormalization of the transport coefficients, e.g. :

$$g_{cs} = \frac{g^0_{cs}}{[1 + (r_c + r_{IS})\ g_{ss}]}. \tag{19}$$

where g_{ss} is the spin conductance of the load (as viewed from the entrance point of the spin current). Detailed calculations will be given elsewhere[23].

Spin leakage is another factor which may occur at each measurement terminal due to spin diffusion. But provided the wires are included in the symmetry considerations, then the symmetry protected setups considered above will clearly remain offset free so that IMR is not affected. The spin leakage will however reduce the signal contrast ΔX. This can be mitigated by having large interface resistances which will hinder spin leakage and ensure that spin accumulation is larger within the load. An extensive discussion will be done elsewhere[23].

We have kept the spin battery in all the discussions at an abstract level. It is important to have realistic setups in mind for experimental checks of our predictions. The spin battery might be operated by ferromagnetic resonance[24], spin Hall effect, spin injection, etc. We give two examples where the spin batteries are built from spin injection using (i) nanopillars and (ii) non-local geometry. Fig. 22 shows a 'bridge' geometry (evidently the bridge should be supported by an insulator) where a nanopillar is used as spin battery (the ferromagnetic layers should be anti-parallel for larger spin voltage); a second nanopillar is used as a load. If the nanopillar to the right is symmetric then one has a parallel IMR. Fig.23 shows a non-local version of the same setup in a planar geometry.

Other interesting setups would be the CIP and CPP ones of Fig. 14 and 17 which are offset free; the CIP

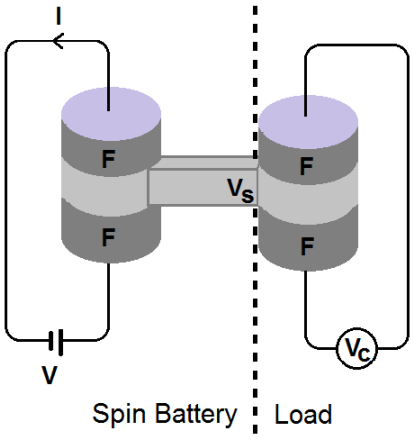

Figure 22. Color online. The spin battery and the load are nanopillar spin valve.

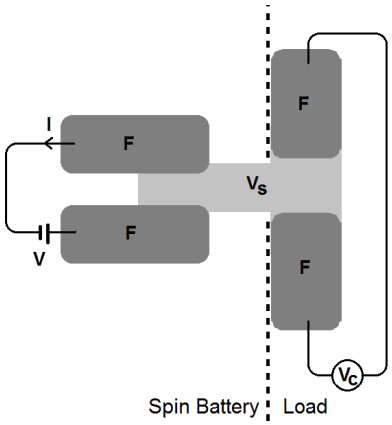

Figure 23. Non local version of the nanopillar setup of Fig.22.

geometry of Fig.17 actually corresponds to two different setups: it can be a layered setup as in standard CIP GMR but the ferromagnetic layers can be thought in the Figure to be parallel to the picture plane. The CPP geometry of 14 also corresponds to several possible setups: a standard layered CPP setup as well as a nanopillar setup and also a non-local setup.

It is not enough to have an IMR it is also important that the non-zero signal is large enough for applications: a large ΔX is necessary (where X is a charge voltage V_c or a current I_c). For instance a mV range for the voltage drop across the load is desirable. To that end it is important to reduce spin backflow, reduce spin leakage in the measurement wires as discussed abvoe, have spin batteries with large spin voltage. A spin battery with small internal spin resistance is therefore preferable since backflow is thus hindered (following Eq. (19)). A small interface resistance between the spin batteries and the load is for the same reason helpful (when compared against the load spin resistance $g_{ss}^{-1} = V_s/I_s$). Having batteries with large spin voltages is an important requirement; ferromagnetic resonance operated batteries yield small spin voltages (spin accumulations are in the μV range typically since the energy scale is given by the resonance frequencies $\propto B$ which cannot be too large). The simplest spin battery relying on spin injection is a single ferromagnet through which a charge current flows. In non-local setups the non-local voltages which scale like the spin accumulation (or spin voltage of the spin battery) are also in the μV range. Through various optimizations (notably the use of large interface resistances to reduce spin leakage) non local voltages have been reported in the $0.1\,mV$ range[25–27]. Further enhancement of the signal can be achieved by connecting more spin batteries to the load. The trilayer spin batteries[23] depicted in Fig.23 or Fig.22 already improve the signal by at least a factor 2), so 4 spin batteries could mean a factor 8 increase. The use of paramagnetic metals with large spin relaxation lengths such as graphene or carbon nanotubes is an interesting prospect in the endeavor to design spin batteries with large spin voltages. In our opinion the mV range is thus probably quite reachable in the near-future.

III. ILLUSTRATIONS.

We illustrate now the IMR effect by considering simple modelings for MTJs (magnetic tunnel junctions), CIP and CPP metallic trilayers.

A. Magnetic tunnel junctions: F-I-F trilayer .

We consider a trilayer F1 | I | F2 connected to two spin batteries in a CPP two-terminal setup (the measurement electrodes are merged with the spin batteries terminals). The geometry is that given in Fig. 14 (with the measurement leads attached to the spin batteries wires; the central layer is the insulator). For identical ferromagnetic layers, the general relation $g_{cs}^{L}(1,\,2) = -g_{cs}^{R}(2,\,1)$ is valid by symmetry.

For simplicity we compute the tunneling current in Jullière model[28] (Slonczewski model[29] yields similar results). Define the DOS polarizations of each ferromagnetic electrode:

$$P_i = \frac{n_{i,+} - n_{i,-}}{n_{i,+} + n_{i,-}}, \tag{20}$$

and the total DOS: $n_i = n_{i,+} + n_{i,-}$. Here $+$ and $-$ refer to majority and minority spin for each layer and *do not refer to an absolute axis.* $\uparrow$ and $\downarrow$ will refer to absolute spin directions. The spin batteries are assumed to be ideal (spin backflow is neglected and we discard contact resistances at the interfaces between spin batteries and the spin valve); the ferromagnetic layers will be assumed to be thin enough for spin accumulation to be uniform (for instance a few nm thick , which is indeed much smaller than $l_{sf} \sim 40 - 60\,nm$ for Co). In other words, *spin flip within the ferromagnets is neglected.* This

hypothesis is not essential, but allows simpler calculations (a more complete calculation will be discussed afterwards at the end of this Section). The spin accumulations are equal to the spin voltages of the battery in contact with the layer considered: for the left layer $V_{sL} = -(\mu_\uparrow - \mu_\downarrow)/2e$ for the chemical potentials in the F1 layer while $V_{sR} = -(\mu_\uparrow - \mu_\downarrow)/2e$ in the layer F2. As in the rest of the paper the spin voltage has a priori a vector dependence: we will for the moment assume it to be parallel to that of the ferromagnet upon which it is applied.

We compute the total tunneling current for each spin species and incorporate angular dependence between magnetizations but we keep spin voltages parallel to the ferromagnetic layer to which they are connected (as in Fig. 16); the magnetization of the right ferromagnet F2 (and the right spin voltage) makes an angle θ with that of the left ferromagnet F1 (and the left spin voltage). The tunneling probability is Γ for $\theta = 0$. We will also neglect all quantum interferences (incoherence approximation). The probabilities of tunneling are then: $\Gamma_{++} = \Gamma \cos^2 \frac{\theta}{2}$, $\Gamma_{+-} = \Gamma \sin^2 \frac{\theta}{2}$, etc, if we assume $|L+\rangle = \cos\frac{\theta}{2}\,|\,R+\rangle + \sin\frac{\theta}{2}\,|\,R-\rangle$ (where $|\,R/L\,\pm\rangle$ are the spin $\pm$ electronic wavefunctions at L or R ferromagnetic electrodes). Then following Slonczewski circuit theory[29] the currents for each spin species entering the junction are:

$$I_{++} = \Gamma \left[n_{1,\uparrow} n_{2,\uparrow} \cos^2 \frac{\theta}{2} \right] (V_c + V_{sL} - V_{sR}), \tag{21}$$

$$I_{+-} = \Gamma \left[n_{1,\uparrow} n_{2,\downarrow} \sin^2 \frac{\theta}{2} \right] (V_c + V_{sL} + V_{sR}),$$

$$I_{--} = \Gamma \left[n_{1,\downarrow} n_{2,\downarrow} \cos^2 \frac{\theta}{2} \right] (V_c - V_{sL} + V_{sR}),$$

$$I_{-+} = \Gamma \left[n_{1,\downarrow} n_{2,\uparrow} \sin^2 \frac{\theta}{2} \right] (V_c - V_{sL} - V_{sR}).$$

Since:

$$n_{1,\uparrow} n_{2,\uparrow} + n_{1,\downarrow} n_{2,\downarrow} = n_1 n_2 \frac{1 + P_1 P_2}{2} \tag{22}$$

$$n_{1,\uparrow} n_{2,\downarrow} + n_{1,\downarrow} n_{2,\uparrow} = n_1 n_2 \frac{1 - P_1 P_2}{2}$$

$$n_{1,\uparrow} n_{2,\downarrow} - n_{1,\downarrow} n_{2,\uparrow} = n_1 n_2 \frac{P_1 - P_2}{2}$$

$$n_{1,\uparrow} n_{2,\uparrow} - n_{1,\downarrow} n_{2,\downarrow} = n_1 n_2 \frac{P_1 + P_2}{2}$$

the total current is eventually:

$$\begin{aligned} I_c = {} & \Gamma n_1 n_2 (1 + P_1 P_2 \cos\theta) V_c \\ & + \Gamma n_1 n_2 (P_1 + P_2 \cos\theta) V_{sL} \\ & - \Gamma n_1 n_2 (P_1 \cos\theta + P_2) V_{sR}. \end{aligned} \tag{23}$$

This implies: $g_c = g_0\ (1 + P_1 P_2 \cos\theta)$, $g_{cs}^L = g_0\ (P_1 + P_2 \cos\theta)$ and $g_{cs}^R = g_0\ (P_1 \cos\theta + P_2)$ where $g_0 = \Gamma n_1 n_2$. The relation $g_{cs}^L(1,\,2) = -g_{cs}^R(2,\,1)$ dictated by symmetry is indeed recovered. Notice the very different ways polarizations enter into the conductances g_c, g_{cs}^L and g_{cs}^R: for the charge conductance the spin valve effect is maximized if $|P_1 P_2|$ is as large as possible, which explains why electrodes as close to half-metals as possible are better as mentioned above (at the end of Section II 4). g_c can only vanish if P_1 and P_2 are equal to ± 1 with $\theta = 0$ or π. For $g_{cs}^{L/R}$ it need not be the case: it vanishes with a weaker condition $P_1 = \pm P_2$ with $\theta = 0$ or π. This results from the fact that the polarizations enter not as a product but additively in g_{cs}. One finds:

- an anti-parallel IMR: for $\theta = 0$ and identical F layers $g_{cs}^L = -g_{cs}^R$, $I_c = g_0\ (P_1 + P_2)\ (V_{sL} - V_{sR}) = g_0\ P\ (\sigma_1 + \sigma_2)\ (V_{sL} - V_{sR})$ where $P = |P_1| = |P_2|$. This vanishes for anti-parallel magnetizations; note that V_{sL} must differ from V_{sR} (otherwise I_c always vanishes whatever the relative orientations). There is no parallel IMR. Note also that $g_{cs}^{L/R}(\sigma_1,\,\sigma_2) = g_{cs}^{L/R}(\sigma_2,\,\sigma_1)$ as expected from systems where spin-flip can be neglected (see Appendix A).

- A non-collinear IMR: to achieve IMR with two spin batteries is much easier than with a single one since the condition is now $0 = g_{cs}^L V_{sL} + g_{cs}^R V_{sR}$ (for $V_c = 0$ or a shorted circuit). By adjusting V_{sR} to obey that condition note that it is no longer necessary to have parallel or anti-parallel magnetizations; for

$$V_{sR} = \frac{P_1 + P_2 \cos\theta}{P_1 \cos\theta + P_2}\, V_{sL} \tag{24}$$

  the current vanishes but once we flip either one of the magnetizations it is non-zero; suppose for instance that $P_1 = P_2 = P$ initially so that the IMR condition on V_{sR} is now $V_{sR} = V_{sL}$; the current $I_c(P_1,\,P_1) = 0$ but if we flip F2 (the angle between magnetizations turning to $\theta + \pi$), the current becomes:

$$I_c(P_1,\,-P_1) = g_0\, 4P\, \sin^2 \frac{\theta}{2}\, V_{sL} \tag{25}$$

  which is largest for $\theta = \pi$ (anti-parallel IMR) and vanishes for $\theta = 0$ (no parallel IMR).

- Note that there is no parallel IMR when spin-flip is neglected because the current for $\theta = 0$ depends only on the difference $V_{sL} - V_{sR}$, $I_c = g_{cs}^L\ (V_{sL} - V_{sR})$ since $g_{cs}^L = g_{cs}^R$ (for $\theta = 0$) so that I_c always vanishes when $V_{sL} = V_{sR}$ whatever the values of P_1 and P_2 (in particular both for $P_1 = P_2$ parallel magnetizations and the opposite $P_1 = -P_2$, that is anti-parallel magnetizations). This is a spurious result which disappears once finite spin relaxation is taken into account in the ferromagnets (see below).

- zero voltage effect: It may be preferable to measure an open-circuit voltage rather than a current. For our junction, an open circuit ($I_c = 0$) implies:

$$V_c = -\frac{P_1 + P_2 \cos\theta}{1 + P_1 P_2 \cos\theta}\, V_s^L + \frac{P_1 \cos\theta + P_2}{1 + P_1 P_2 \cos\theta}\, V_s^R \tag{26}$$

For identical ferromagnets $P_1 = P_2$ and $\theta = 0$, note that the voltage V_c is of the same order of magnitude as the spin voltage V_s^L since $\partial V_c/\partial V_{sL}$ reaches quickly to 1 when P increases; for instance for $P = 0.5$, $\partial V_c/\partial V_{sL} = 0.8$, while for $P = 0.75$ (as in Co for CPP GMR), $\partial V_c/\partial V_{sL} = 0.96$.

The previous results are valid only if there are no offsets (due for instance to heat currents, Seebeck effects ...) and if spin-flip is negligible. If one incorporates spin relaxation within the ferromagnetic layers, the relation $g_{cs}^L = g_{cs}^R$ for collinear settings is no longer valid. For a symmetric MTJ with identical coupling to two spin batteries, the discussion for symmetric CPP trilayers of Section II 5 applies; for instance in the limit of short ferromagnetic layers (thickness much smaller than the spin relaxation length), one finds:

- an anti-parallel IMR for $V_{sL} = -V_{sR}$ with vanishing anti-parallel current $I_c^{\nparallel} = I_c\,(P_1, -P_1) = 0$ but a non zero parallel current

$$I_c^{\parallel} = I_c\,(P_1, P_1) = 4\,g_0\,P_1\,V_{sL} \tag{27}$$

to lowest order in d_F/l_F (thickness of ferromagnetic layers over spin relaxation length). By symmetry there are no offsets so that $I_c^{\nparallel}$ definitely vanishes.

- a parallel IMR for $V_{sL} = V_{sR}$ with $I_c^{\parallel} = 0$ but

$$I_c^{\nparallel} \propto \frac{d_F}{l_F}\,g_0^2\,r_F\,P_F^3\ \ \left(1 - P_1^2\right)V_{sL} \tag{28}$$

which vanishes when spin-flip is neglected (so that there is no parallel IMR any more as discussed above); r_F and P_F are the spin resistance and conductivity polarizations of the ferromagnet ($r_F = \rho_F^*\,l_F/A$ with usual GMR notations) while P_1 is the DOS polarization of ferromagnet $F1$. The parallel IMR is offset free again by symmetry but is much weaker than the anti-parallel IMR (namely, $\Delta I_c = I_c^{\parallel} - I_c^{\nparallel}$ is much smaller for parallel IMR).

A more elaborate modeling including measurement leads, spin leakage, interface resistances as well as internal spin resistances does not modify substantially these results. These effects do however reduce the response ΔI_c or ΔV_c so for practical uses it is of interest to study them; other interesting effects such as Spin Transfer Torque will be discussed extensively elsewhere[23].

B. CIP metallic spin valves .

A precise modeling in CIP structure is quite involved because of spin accumulation. We will satisfy ourselves in this introductory paper with simple resistor models which are crude but yield interesting insights. Since we adopt a two-channel point of view, it makes no difference to consider a single or two spin batteries. Indeed within a two-channel model with a two-terminal geometry (merging measurement electrodes with spin batteries wires) the current is easily shown to depend only on the difference $V_{sL} - V_{sR}$: $I_c = g_c\,V_c + g_{cs}\,(V_{sL} - V_{sR})$ where $g_c = g_\uparrow + g_\downarrow$ and $g_{cs} = g_\uparrow - g_\downarrow$ if V_{sL} is a spin voltage applied to the left terminal and V_{sR} a spin voltage applied to the right terminal. In practice however the best CIP setup is that of Fig. 17 which is offset protected by symmetry when $V_{sL} = -V_{sR}$.

1. *Large mean free path.*

This is normally the limit applicable to metallic multilayers where the mean free path is typically between tens or hundreds of interatomic distances. In that limit Mathon has argued from a Boltzmann's equation approach that electrons experience an average resistivity[30], which for two layers of width a and b is $\overline{\rho} = [a\rho_a + b\rho_b]/(a+b)$. Although the proof is not valid stricto sensu in our context we will adopt the assumption at least as a rough starting point.

Let us consider a F - N - F trilayer; then:

$$\rho_{\sigma=\uparrow,\downarrow} = \frac{d_1\rho_{1,\sigma} + d_2\rho_{2,\sigma} + d_N\rho_N}{w} \tag{29}$$

where $w = d_1 + d_2 + d_N$ and $\rho_{i,\sigma}$is the resistivity in layer i for spin σ, ρ_N being the resistivity of the normal layer. The conductances of each spin channel are:

$$g_\sigma = \frac{1}{r_\sigma} = \frac{A\,w}{L\,(d_1\rho_{1,\sigma} + d_2\rho_{2,\sigma} + d_N\rho_N)} \tag{30}$$

where L is the length of the CIP multilayers, and A is the lateral area. Let us introduce polarizations per:

$$P_i = \frac{\rho_\downarrow - \rho_\uparrow}{\rho_\downarrow + \rho_\uparrow}\ \left(= \frac{\sigma_\uparrow - \sigma_\downarrow}{\sigma_\uparrow + \sigma_\downarrow}\right) \tag{31}$$

and $\rho_i = \rho_{i,\downarrow} + \rho_{i,\uparrow}$. The charge conductance g_c and charge-spin conductance g_{cs} are

$$g_c = g_\uparrow + g_\downarrow = \frac{4A\,w}{L}\,\frac{(d_1\rho_1 + d_2\rho_2 + 2d_N\rho_N)}{(d_1\rho_1 + d_2\rho_2 + 2d_N\rho_N)^2 - (d_1\rho_1 P_1 + d_2\rho_2 P_2)^2} \tag{32}$$

$$g_{cs} = g_\uparrow - g_\downarrow = \frac{4A\,w}{L}\,\frac{(d_1\rho_1 P_1 + d_2\rho_2 P_2)}{(d_1\rho_1 + d_2\rho_2 + 2d_N\rho_N)^2 - (d_1\rho_1 P_1 + d_2\rho_2 P_2)^2} \tag{33}$$

which is odd in P_i as it should be (see Section II 2) while g_c exhibit the usual GMR.

Polarity change: suppose $|d_1\rho_1 P_1| > |d_2\rho_2 P_2|$; then reverse the magnetization of layer 1: $P_1 \to -P_1$; it follows that g_{cs} will change its sign.

IMR: if however $|d_1\rho_1 P_1| = |d_2\rho_2 P_2|$ by reversing any of the ferromagnetic layers we end up with a zero conductance, and therefore a zero current, if initially the conductance was non-zero. This is an anti-parallel IMR.

As discussed in Section II 5, in order to actually observe IMR in this CIP geometry, it is necessary to add a second spin battery which enables cancellation of possible offsets by relying on symmetry (Figs. 17 - 18).

2. Short mean free path.

The opposite (dirty) limit: $\lambda \ll d_i$ is quite interesting on the theoretical level (though we leave open the discussion of the practical use) because there is no GMR for the charge response in this limit but yet we have an IMR for the response to spin batteries. In that limit we can consider that conduction in each layer is in parallel (perfect partition): due to the small mean free path we take as a zero order approximation that very few electrons travel across layers. (One might add interface resistances, but they don't change drastically the end results).

$$g_\uparrow = \frac{A}{l}\,\left(\sigma_{1,\uparrow} + \sigma_{2,\uparrow} + \frac{\sigma_N}{2}\right) \tag{34}$$

and a likewise expression for $g_\downarrow$. As a result there is no GMR since

$$g_c = g_\uparrow + g_\downarrow = \frac{A}{l}\,(\sigma_1 + \sigma_2 + \sigma_N) \tag{35}$$

doesn't depend on the relative orientation of layer 1 and 2 ($\sigma_i = \sigma_{i,\uparrow} + \sigma_{i,\uparrow}$).

However:

$$g_{cs} = g_\uparrow - g_\downarrow = \frac{A}{l}\,(\sigma_1 P_1 + \sigma_2 P_2) \tag{36}$$

which does exhibit the IMR effect.

Polarity change: suppose $|\sigma_1 P_1| > |\sigma_2 P_2|$; then reverse the magnetization of layer 1: $P_1 \to -P_1$; it follows that $g_{cs} \to -g_{cs}$; there is a current reversal.

IMR: if the ferromagnetic layers are identical then

$$g_{cs} = \frac{A\,\sigma_F}{l}\,(P_1 + P_2) \tag{37}$$

which is the familiar expression, odd in $P_1 + P_2$ and exhibiting anti-parallel IMR. (There is no parallel IMR.)

More detailed modeling of spin voltage driven CIP spin valves involves CPP characteristics since there is a spin accumulation: however the general discussion of Section II shows that the main results (IMR) will not be affected.

3. Angular dependence.

As a rough order zero calculation we can compute the angular dependence when there is an angle between the magnetizations of the two ferromagnetic layers while keeping the spin voltages in a reference direction identical to that of one of the layers (for instance layer 1). We assume additive scattering rates as well as incoherence so that in layer 2 for each spin species:

$$\frac{1}{\tau_\sigma(\theta)} = \frac{\cos^2(\theta/2)}{\tau_\sigma(0)} + \frac{\sin^2(\theta/2)}{\tau_{-\sigma}(0)} \tag{38}$$

so that

$$\sigma_{2,\uparrow}(\theta) = \sigma_{2,\uparrow}(0)\,\cos^2\left(\frac{\theta}{2}\right) + \sigma_{2,\downarrow}(0)\,\sin^2\left(\frac{\theta}{2}\right) \tag{39}$$

and a similar expression for $\sigma_{2,\downarrow}(\theta)$. This is probably more correct in the limit of short mean free path where conductances for each spin species can be added, while in the opposite limit, one adds the resistances. For short mean free path, one gets:

$$g_{cs}(\theta) = \frac{A\,\sigma_F}{l}\,(P_1 + P_2\,\cos(\theta))\,. \tag{40}$$

(But in addition to this regular response, there may be offsets since the setup is not symmetry-protected against them.)

C. CPP Metallic spin valves .

We consider a CPP trilayer connected to two ideal spin batteries with spin voltages V_{sL} and V_{sR}. The measurement probes are merged with the batteries wires so that one has a two-terminal geometry (see Fig. 14 modified by shifting terminals $T1$ and $T2$ to the spin batteries). For simplicity, spin current continuity is assumed at interfaces (no spin flip at interfaces); the chemical potentials are discontinuous at interfaces due to contact resistances and we introduce $r_{ci} = (r_{c,i\uparrow} + r_{c,i\downarrow})/4$ and

$P_{ci} = -\left(r_{c,i\uparrow} - r_{c,i\downarrow}\right)/r_{ci}$ (conductance polarization $= \gamma$ in Valet-Fert notation) for each F-N interface ($i = 1, 2$ for the left and right interfaces respectively). But we neglect interface resistances at the spin batteries contact with the ferromagnets. A more realistic modeling including spin leakage at measurement terminals, internal spin resistance of the batteries as well as interface resistances does not modify substantially the results.

Each ferromagnetic layer has width d_i, spin diffusion length l_i , spin resistance $r_i = l_1\ \left(\rho_{1,\uparrow} + \rho_{1,\downarrow}\right)/A$ (A is the section) and P_i is the conductivity polarization ($= \beta$ in Valet-Fert notations). The paramagnetic N layer has width d_N, spin relaxation length l_N, spin resistance r_N. We also define: $\cosh_{1/2/N} = \cosh\frac{d_{1/2/N}}{l_{1/2/N}}$ (likewise for $\sinh_{1/2/N}$).

Using the standard drift-diffusion equations[4–6] after tedious calculations one ends up with the expressions of $V_c = k_{cs}^L\, V_{sL} + k_{cs}^R\, V_{sR}$.

Defining:

$$\begin{aligned}\Delta = {} & r_N \cosh_N \left[\cosh_1 r_2 \sinh_2 + \cosh_2 r_1 \sinh_1 + (r_{c1} + r_{c2}) \cosh_1 \cosh_2\right] \\ & + \sinh_N \left[r_N^2 \cosh_1 \cosh_2 + (r_1 \sinh_1 + r_{c1} \cosh_1)\,(r_2 \sinh_2 + r_{c2} \cosh_2)\right]\end{aligned}$$

one finds:

$$\begin{aligned}k_{cs}^L \times \Delta = {} & P_1 \left\{r_N \cosh_N \left[r_2 \sinh_2 + (r_{c2} + r_2) \cosh_2\right] + \sinh_N \left[r_N^2 \cosh_2 + r_{c1}\,(r_2 \sinh_2 + r_{c2} \cosh_2)\right] - \Delta\right\} \\ & - \ P_{c1} r_{c1} \left[r_N \cosh_N \cosh_2 + \sinh_N\,(r_2 \sinh_2 + r_{c2} \cosh_2)\right] - r_N \left[P_2 r_2 \sinh_2 + P_{c2} r_{c2} \cosh_2\right] \qquad (41)\end{aligned}$$

and $k_{cs}^R = -k_{cs}^L\ (1 \longleftrightarrow 2)$. The conductances $g_{cs}^{L/R}$ follow by multiplying by (minus) the charge conductance $-g_c$.

For F layers identical in all respects (except for the direction of their magnetization indexed by $\sigma_i = \pm 1$), it is readily checked that: $k_{cs}^L(\sigma_1,\, \sigma_2) = -k_{cs}^R(\sigma_2,\, \sigma_1)$. We have explicitly recovered parallel IMR for $V_{sL} = V_{sR}$ and anti-parallel IMR for $V_{sL} = -V_{sR}$ as surmised in Section II 5 through general arguments.

Non-collinear conductances can be computed using magnetoelectronic circuit theory[7]; one finds for identical layers:

$$g_{cs}^L \propto \frac{a + b\,\cos^2(\theta/2)}{a + b\,\cos^2(\theta/2) + \sin^2(\theta/2)} \qquad (42)$$

where a and b are material dependent constants (related in particular to the spin-mixing conductance), θ is the angle between the ferromagnet magnetizations and the left and right spin voltages are assumed parallel to respectively the left and right ferromagnet magnetizations. More importantly one finds $g_{cs}^L = -g_{cs}^R$ which implies non-collinear IMR is achieved for $V_{sL} = V_{sR}$ (the spin voltages are assumed to be measured against the direction of the ferromagnets (see Section II 5) so that the condition $V_{sL} = V_{sR}$ is not exclusive to parallel IMR in this context). Details will be discussed elsewhere[23] but the results again confirm the analysis of Section II 5.

IV. CONCLUSION AND PROSPECTS.

We have shown that spin valves driven by spin batteries may exhibit infinite magnetoresistance which come in three flavors: parallel IMR, anti-parallel IMR and non-collinear IMR whereby magnetoresistance is infinite for parallel, anti-parallel or non-collinear magnetizations while it stays finite if one switches one of the two magnetic regions of the load. A distinctive feature of spin battery driven IMR is that it is not a material dependent effect while for standard GMR one would need half-metals to convert it into an IMR; it requires however symmetrical setups which will ensure protection against possible offsets (of thermal origin essentially). A (symmetric) spin valve is therefore a perfect spin transistor when driven by one spin battery (or two spin batteries). The IMR effect of spin valves can in a sense be understood as just a variant of the bipolar response of Johnson transistor, with the important practical distinction that offsets can be circumvented.

Explicit calculations for several geometries confirm the general analysis based on symmetries. For CPP MTJ in Jullière model and Slonczewski circuit theory one recovers the various IMR effects; anti-parallel IMR is found to be much stronger than parallel IMR and non-collinear IMR. CIP spin valves have been predicted to display IMR even in the dirty limit (mean free path smaller than the layers widths) in contrast with CIP trilayers driven by charge batteries. The charge response to two spin batteries has also been computed for a CPP metallic spin valve; but IMR can readily be observed when a single spin battery is connected to the normal layer of a symmetric CPP metallic trilayer.

In terms of practical applications, the notion of an IMR is certainly inviting for all the range of devices relying on GMR and wherever there is a use for a perfect spin transistor. Whether IMR will actually prove useful will require further experimental investigations; a key component will be in particular the search for spin batteries outputting sufficiently large spin voltages to allow practical use.

ACKNOWLEDGMENTS

The author thanks F. Piéchon and N. Vernier for useful discussions.

Appendix A: CPP spin valves in the absence of spin flips.

We consider a trilayer in the geometry depicted in Fig. 24: we assume (1) identical F layers (same width, same material and geometry), (2) spin-flip can be neglected (widths much smaller than the spin relaxation lengths), (3) the measurement terminals T_1 and T_2 are each in symmetrical contact with layers F1 and F2 respectfully, (4) the spin battery is positioned asymmetrically with respect to the F layers (so that parallel IMR is prevented). Then $g_{cs}(\sigma_2,\,\sigma_1) = g_{cs}(\sigma_1,\,\sigma_2)$. Indeed in the absence of spin-flip one has a two-channel model with conductances $g_\uparrow$ and $g_\downarrow$ between terminals $T1$ and $T2$ which are assumed to be shorted so that the voltage drop between them vanishes ($V_c = 0$). Currents for each channel are then:

$$I_\uparrow = g_\uparrow\,(V_{\uparrow 1} - V_{\uparrow 2})\,, \tag{A1}$$
$$I_\downarrow = g_\downarrow\,(V_{\downarrow 1} - V_{\downarrow 2})\,. \tag{A2}$$

The spin accumulations at each terminal are proportional to V_s the spin voltage of the spin battery so that $(V_{\uparrow 1} - V_{\uparrow 2})/V_s$ is a non-vanishing geometry dependent constant C (independent of V_s); since $V_{\uparrow i} = -V_{\downarrow i}$ (zero charge voltage at each terminal when they are shorted), one has also $C = -(V_{\downarrow 1} - V_{\downarrow 2})/V_s$. Therefore:

$$I_\uparrow = g_{\uparrow eff}\,V_s, \tag{A3}$$
$$I_\downarrow = -g_{\downarrow eff}\,V_s. \tag{A4}$$

where we have defined effective channel conductances: $g_{\sigma eff} = g_\sigma\,C$. We can write for each spin conductance $g_\uparrow(\sigma_1,\,\sigma_2) = [r(\sigma_1) + r(\sigma_2)]^{-1}$ and $g_\downarrow(\sigma_1,\,\sigma_2) = [r(-\sigma_1) + r(-\sigma_2)]^{-1}$ since the layers are identical. This implies $g_{\uparrow eff}(\sigma,\,\tau) = g_{\uparrow eff}(\tau,\,\sigma)$. Therefore $g_{cs} = (g_{\uparrow eff} - g_{\downarrow eff})$ obeys the condition $g_{cs}(\sigma_2,\,\sigma_1) = g_{cs}(\sigma_1,\,\sigma_2)$ which in turn implies the possibility of an anti-parallel IMR.

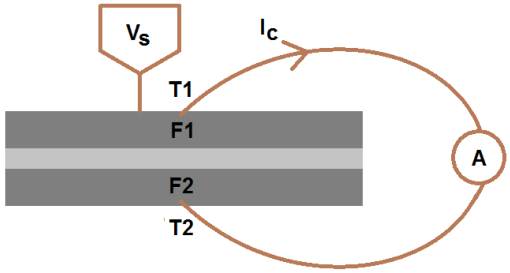

Figure 24. Color online. Trilayer in CPP geometry. Spin battery is not positioned in any symmetric position with respect to the ferromagnetic layers.

An example is provided by CPP MTJ in Jullière model[28] since spin-flip is discarded in the F layers. Therefore the relation $g_{cs}(\sigma_2,\,\sigma_1) = g_{cs}(\sigma_1,\,\sigma_2)$ must be obeyed (this was also shown directly in section III A).

* pham@lps.u-psud.fr

[1] B. Dieny, V. S. Speriosu, S. S. P. Parkin, B. A. Gurney, D. R. Wilhoit, and D. Mauri, Physical Review B **43**, 1297 (1991).
[2] C. Chappert, A. Fert, and F. N. Van Dau, Nat Mater **6**, 813 (2007).
[3] A. G. Aronov, JETP Lett. **24**, 32 (1976).
[4] M. Johnson and R. H. Silsbee, Physical Review B **35**, 4959 (1987).
[5] T. Valet and A. Fert, Physical Review B **48**, 7099 (1993).
[6] E. Rashba, The European Physical Journal B - Condensed Matter **29**, 513 (2002).
[7] A. Brataas, Y. V. Nazarov, and G. E. W. Bauer, Physical Review Letters **84**, 2481 (2000).
[8] M. Johnson and R. H. Silsbee, Physical Review B **76**, 153107 (2007).
[9] A. Fert, J. George, H. Jaffres, and R. Mattana, IEEE Transactions on Electron Devices **54**, 921 (2007).
[10] M. Johnson, Science **260**, 320 (1993).
[11] M. Ichimura, Journal of Applied Physics **95**, 7255 (2004).
[12] J. Hamrle, T. Kimura, Y. Otani, K. Tsukagoshi, and Y. Aoyagi, Physical Review B **71**, 094402 (2005).
[13] J. Hamrle, T. Kimura, T. Yang, and Y. Otani, Journal of Applied Physics **98**, 064301 (2005).
[14] S. Garzon, I. Zutic, and R. A. Webb, Physical Review Letters **94**, 176601 (2005).
[15] F. Casanova, A. Sharoni, M. Erekhinsky, and I. K. Schuller, Physical Review B **79**, 184415 (2009).
[16] F. L. Bakker, A. Slachter, J.-P. Adam, and B. J. van Wees, Physical Review Letters **105**, 136601 (2010).
[17] M. Johnson and R. H. Silsbee, Physical Review B **37**, 5312 (1988).
[18] M. Johnson and R. H. Silsbee, Physical Review Letters **55**, 1790 (1985).
[19] J. Bass and W. P. Pratt, Journal of Physics: Condensed Matter **19**, 183201 (2007).
[20] M. Johnson, Physical Review Letters **70**, 2142 (1993).
[21] J.-M. George, A. Fert, and G. Faini, Physical Review B **67**, 012410 (2003).
[22] T. Kimura and Y. Otani, Physical Review Letters **99**, 196604 (2007).
[23] K.-V. Pham, unpublished (2016).
[24] A. Brataas, Y. Tserkovnyak, G. E. W. Bauer, and B. I. Halperin, Physical Review B **66**, 060404 (2002).
[25] T. Wakamura, K. Ohnishi, Y. Niimi, and Y. Otani, Applied Physics Express **4**, 063002 (2011).
[26] Y. Fukuma, L. Wang, H. Idzuchi, S. Takahashi, S. Maekawa, and Y. Otani, Nat Mater **10**, 527 (2011).

[27] Y. Fukuma, L. Wang, H. Idzuchi, and Y. Otani, Applied Physics Letters **97**, 012507 (2010).
[28] M. Julliere, Physics Letters A **54**, 225 (1975).
[29] J. C. Slonczewski, Physical Review B **39**, 6995 (1989).
[30] D. Edwards, J. Mathon, and R. Muniz, IEEE Transactions on Magnetics **27**, 3548 (1991).